

## Unstable periodic orbits in human cardiac rhythms

K. Narayanan, R. B. Govindan, and M. S. Gopinathan\*

*Department of Chemistry, Indian Institute of Technology, Madras 600 036, Chennai, India*

(Received 4 November 1997)

Unstable periodic orbits (UPOs) extracted from experimental electrocardiograph signals are reported for normal and pathological human cardiac rhythms. The periodicity and distribution of the orbits on the chaotic attractor are found to be indicative of the state of health of the cardiac system. The normal cardiac system is characterized by three to four UPOs with typical periodicities and intensities. However, pathological conditions such as premature ventricular contraction, atrio ventricular block, ventricular tachy arrhythmia, and ventricular fibrillation have UPOs whose periodicity and intensity distribution are quite distinct from those of the healthy cases and are characteristic of the pathological conditions. Eigenvalues and the largest positive Lyapunov exponent value for the UPOs are also reported. The UPOs are shown to be insensitive to the embedding dimension and the present UPO analysis is demonstrated to be reliable by the method of surrogate analysis. [S1063-651X(98)05904-2]

PACS number(s): 87.10.+e, 05.45.+b

### I. INTRODUCTION

The detection of unstable periodic orbits (UPOs) in experimental data has emerged as an important issue in current studies of chaotic dynamics [1–5]. Even though the trajectories in a chaotic attractor have in principle infinite periodicity, the attractor is dominated by a limited number of UPOs [6]. The importance of determining the UPOs arises from the fact that the invariant properties of the attractor such as its entropy, Lyapunov spectrum, and dimensions can be expressed in terms of the UPOs [7–9]. Moreover, the possibility of extraction of UPOs in an experimental system is evidence for the existence of determinism in its dynamics [10]. From a practical point of view, chaos control techniques [11–18] can be implemented judiciously if the UPOs of a system are known.

In this article we report the UPOs of the human cardiac system for some typically normal healthy and pathological cases. The UPOs are extracted from the chaotic attractor constructed from measured electrocardiograph (ECG) signals. It turns out that the human cardiac system behaves as a deterministic chaotic system with a limited number of dominant UPOs. The number of significant UPOs and their density distribution are found, in this preliminary study, to be characteristic of the condition of normalcy and pathology of the heart. However, properties such as the correlation dimension of the attractor and the eigenvalues or the Lyapunov exponents of the UPOs and of the attractor do not show such a distinction.

For physiological systems such as the cardiac system, it is generally difficult to confirm the presence of deterministic chaos from the usual dimensional analysis [19]. Analysis of ECG signals based on nonlinear dynamical measures such as correlation dimension, Lyapunov exponents, and Kolmogorov entropy has indicated that the dynamics of the cardiac system is deterministic chaos [20,21]. Varying estimates of the correlation dimension ranging from 3.6 to 5.2 [20] and

from 2.1 to 3.2 [21] have been reported. The correlation dimension estimated at different portions of the time series varies for pathological subjects, whereas there is repeatability in the case of normal subjects [21]. However, the determination and interpretation of dimensions and exponents from experimental data is subject to several limitations, especially in the presence of noise, and this is an area of active current research [22–24]. The control of cardiac chaos by identifying the stable and unstable directions about a saddle point and applying timely perturbation also has been successfully implemented by cardiac cell preparations [25]. Recently, a dynamic control technique to control the alternans rhythm [26] has been developed, which may have important clinical implications.

The *recurrence* method for extraction of UPOs from experimental data is well documented [7] and it has been applied to data from the Belousov-Zhabotinsky reaction [6] and a chaotic laser solid-state system [27]. More recently, UPOs have been extracted by suitable transformation of the time series and have been successfully applied to experimental chaotic data from a gravitationally buckled magnetoelastic ribbon system [10] and neuronal ensemble from mammalian brain slices [28]. In this article we employ the recurrence method of Ref. [6] to extract UPOs of the cardiac system. The procedure consists briefly of first constructing the attractor from the time series by the method of delay coordinates with a proper choice of embedding dimension  $d$  and delay time  $\tau$  [29]. Then taking the point  $\mathbf{x}_i$  on the attractor, the dynamical steps are followed as  $\mathbf{x}_{i+1}, \mathbf{x}_{i+2}, \dots, \mathbf{x}_j$  until we find the smallest index  $j > i$  such that  $\|\mathbf{x}_i - \mathbf{x}_j\| < \varepsilon$ , where  $\varepsilon > 0$  is a small predetermined distance below which two points on the attractor are considered to be coincident. If such a  $j$  exists, we then define  $m = j - i$  and represent  $\mathbf{x}_i$  as an  $(m, \varepsilon)$  recurrent point. The procedure is repeated for all points  $i = 1, \dots, N$  on the attractor.

### II. UPOs OF LORENZ AND RÖSSLER SYSTEMS

Before applying the method to the study of ECG time series, we investigate the UPOs for the standard chaotic sys-

\*Electronic address: msgopi@hotmail.com

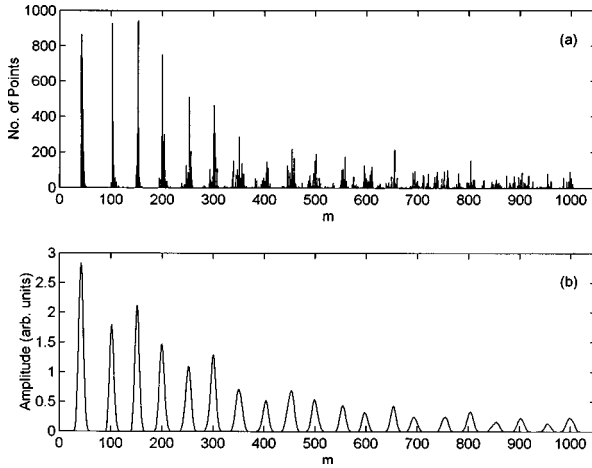


FIG. 1. UPOs for the Lorenz attractor: (a) histogram and (b) its convolution.  $m$  is the recurrence number of the UPO with  $m=1$  corresponding to 0.01 time unit. See Table I for relative intensities of the UPOs.

tems, the Lorenz and Rössler attractors with the parameter values  $(R, \sigma, b) = (40, 16, 4)$  for the Lorenz system and  $(a, b, c) = (0.2, 0.2, 5.7)$  for the Rössler system.

In previous works [1,4], the UPOs of the Lorenz and Rössler systems were extracted by constructing the Poincaré section.

Figure 1(a) shows the histogram obtained for the UPOs of the Lorenz attractor, where the number of  $(m, \varepsilon)$  points are plotted against  $m$ . The Lorenz attractor is found to consist of 20 significant UPOs (see Table I) with a basic periodicity of  $m=50$ , others being integral multiples of this periodicity. This is more clearly seen when the histogram is convoluted with a Gaussian response function of width  $m=4$ , as shown in Fig. 1(b). The sum of the areas under the peaks for the entire attractor is normalized to 100 for convenience. Since the integration step size is 0.01, the basic periodicity corresponds to 0.5 of a time unit. The UPOs, their relative weights, and their eigenvalues are reported in Table I.

The stability of the individual UPOs is estimated from a linear approximation of the dynamics at points on nearby trajectories (see Ref. [6] for details of the calculation of the transformation matrix  $A$ , which takes  $\mathbf{x}_i$  to  $\mathbf{x}_{i+m}$ ). The transformation matrix  $A$  is an approximation of the Jacobian matrix. The absolute value of the largest eigenvalue of  $A$  gives the strength of repulsion of the saddle orbit near  $\mathbf{x}_i$ . It is important to observe that nearly 95% of the attractor points belong to these UPOs, confirming that UPO analysis of the chaotic attractor is reliable. For example, we also report in Table I the largest Lyapunov exponent  $\lambda$  calculated for the entire Lorenz attractor as a weighted sum of the exponent of the individual UPOs. This is seen to be in reasonable agreement with the exact value directly calculated for the whole attractor [30]:  $\lambda = 2.16$  bits/sec.

Similar results are obtained for the Rössler attractor too. The attractor is well represented by 12 (note that period 4 is absent) significant UPOs (Fig. 2). The Lyapunov exponent estimated from the UPOs is again in agreement with the exact values [30]:  $\lambda = 0.13$  bits/sec.

### III. HUMAN CARDIAC SYSTEM AS CHAOTIC

Having gained confidence in the methodology of UPOs to describe well-known chaotic attractors, we now proceed to

TABLE I. UPOs for Lorenz and Rössler attractors reconstructed from  $x(t)$  time series of 40 000 and 10 000 points with delay times  $\tau$  of 0.10 and 1.2 and step sizes 0.01 and 0.12, respectively.  $\varepsilon = 0.02$  for the Lorenz system and  $\varepsilon = 0.03$  for the Rössler system. Here  $p$  is the period,  $w$  is the weight (in %),  $e$  is the eigenvalue, and  $\lambda$  is the largest positive Lyapunov exponent in bits/sec.

Lorenz			Rössler		
$p$	$w$	$e$	$p$	$w$	$e$
1	17	2.63	1	4	5.18
2	10	22.84	2	3	8.67
3	12	27.78	3	48	13.02
4	9	18.33	5	9	7.81
5	7	13.13	6	5	11.04
6	8	12.27	7	2	8.04
7	5	9.85	8	12	10.37
8	3	11.04	9	2	9.57
9	5	16.07	10	6	10.94
10	4	9.22	11	7	55.46
11	3	12.52	12	1	70.46
12	2	18.98	13	1	3.34
13	3	11.24			
14	2	9.03			
15	2	8.07			
16	2	11.26			
17	1	18.03			
18	2	18.35			
19	1	5.97			
20	2	14.53			
	$\langle \lambda \rangle$	2.19		$\langle \lambda \rangle$	0.12

study the UPOs of the human cardiac system from its measured ECG time series.

Unlike the theoretical systems analyzed above, the experimental system presents several difficulties. The embedding dimension is not known *a priori* and the estimates of the invariants of the attractor are sensitive to noise that is always present in the measurement process. These problems have

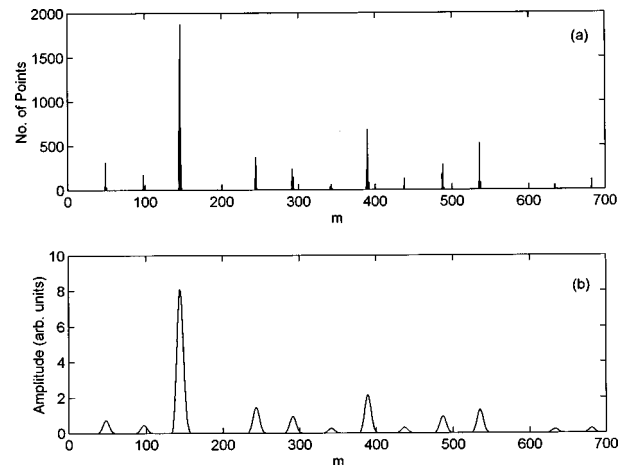


FIG. 2. UPOs for the Rössler attractor: (a) histogram and (b) its convolution.  $m$  is the recurrence number of the UPO with  $m=1$  corresponding to 0.12 time unit. See Table I for relative intensities of the UPOs.

been addressed by several authors [31–34]. In order to suppress noise in the ECG time series measured at 360 Hz, we filtered the ECG time series between 0.5 and 45 Hz and down sampled to 90 Hz. After down sampling, we normalized it between 0 and 1 to extract the UPOs. We took 10 000 points each for normal, premature ventricular contraction (PVC), and atrio ventricular (AV) block and 14 000 points each for ventricular tachy arrhythmia (VTA) and ventricular fibrillation (VF).

The embedding dimension  $d$  for the experimental attractor is decided by the standard method [35] of estimating the correlation dimension  $d_2$  as a function of the embedding dimension and looking for saturation of  $d_2$ . In all cases,  $d_2$  essentially saturates around 2–2.8, except for VF, in which case it saturates around 5–6. For the sake of comparison, we take the embedding dimension to be 3 in all the cases for further studies reported here.

To make certain that we are dealing with deterministic chaos, we have done a short-term predictability analysis to the ECG time series by the method proposed by Lefebvre *et al.* [36], which is a modification of Sugihara and May’s method [37]. By the term “deterministic chaos” we imply that the system must be predictable for a short period of time. For a chaotic system the correlation coefficient  $\rho$  between the actual values and the predicted values falls to near zero as the prediction time  $P$  is increased [37].

We have applied the short-term prediction analysis for both the normal and pathological time series. In all the cases, the correlation coefficient  $\rho$  falls to zero as the prediction time  $P$  is increased, which indicates the chaotic nature of the ECG time series. Refer to [38] for details of the prediction analysis.

The presence of a nonlinear structure in the ECG time series can be established by performing surrogate data analysis [39,40]. This analysis has been applied to the ECG time series using both the random-phase and Gaussian-scaled random-phase surrogates. These surrogates will destroy the nonlinear structure, if any, present in the time series. Since the original and the surrogate data sets will have the same linear properties, any difference in the discriminating metric between the original and the surrogate must be only because of the nonlinear structure present in the original time series. The significance  $S$ , defined as  $S = (\langle D_{\text{sur}} \rangle - D_{\text{ori}}) / \sigma$  (where  $D_{\text{sur}}$  and  $D_{\text{ori}}$  are the values obtained for surrogate and original using correlation dimension  $d_2$  as the discriminating metric, angular brackets represent the mean, and  $\sigma$  is the standard deviation of the  $D_{\text{sur}}$ ), has been calculated for the normal, PVC, VTA, AV block, and VF cases. The values are  $65 \pm 0.2$ ,  $181.1 \pm 1.8$ ,  $52.7 \pm 0.1$ ,  $100.1 \pm 0.3$ , and  $5.2 \pm 0.1$ , respectively, for the phase-randomized surrogates [38]. Similarly for Gaussian-scaled surrogates, the values are  $33.5 \pm 0.2$ ,  $24.4 \pm 0.1$ ,  $19 \pm 0.1$ ,  $25.2 \pm 0.1$ , and  $5.76 \pm 0.1$ , respectively [38] (see Ref. [38] for details of the analysis of surrogate data). The sharp fall in the correlation coefficient  $\rho$  with the prediction time  $P$ , the saturation of correlation dimension  $d_2$  as a function of embedding dimension, and the presence of nonlinear structure inferred from the surrogate data analysis point to the fact that ECG time series is deterministically chaotic.

#### IV. UPOs OF THE HUMAN CARDIAC SYSTEM

We recorded ECGs for normal healthy people using volunteers with a 12-bit analog-to-digital converter sampled at a rate of 360 Hz. ECGs for pathological subjects were taken from the MIT-BIH arrhythmia database [41]. All the pathological subjects were sampled at 360 Hz, except those with VTA and VF, which were sampled at 250 Hz.

Figures 3(a)–3(e) show three-dimensional views of the chaotic attractor for a typically normal and pathological cases such as PVC, VTA, AV block, and VF, respectively, along with the ECG time series and their power spectra. Even though ECGs for the normal and these pathological cases can be distinguished qualitatively by a trained physician, neither the power spectrum nor the dimension estimation can provide much additional information. However, the situation turns out to be quite different when we consider the UPOs.

We have determined the UPOs for the cardiac rhythm by the recurrence procedure outlined above, for several young healthy (ten cases), old healthy (ten cases), and different pathological PVC (six cases), AV block (two cases), VTA (four cases), and VF (four cases) cases. These are summarized in Table II, where the periodicity  $p$ , weight  $w$  (in %), eigenvalue  $e$ , and largest positive Lyapunov exponent  $\lambda$  are given. Table II also lists (in column 1) the delay time  $\tau$  and radius  $\varepsilon$  used in the extraction of UPOs for all cases. The UPO distribution is essentially insensitive to the variation of  $\varepsilon$  within 10% of the reported values in Tables I and II. Generally  $\sim 80\%$  of the number of attractor points are found to belong to the dominant UPOs of the attractor for this choice of  $\varepsilon$ .

The histogram for a typical healthy case and its convolution with the Gaussian response function of width 4 is shown in Figs. 4(a) and 4(b). Typical trajectories for period 1 and 2 of a normal subject and a PVC subject are shown in Figs. 5(a)–5(d).

There are three to four dominant UPOs in the young normal (healthy) individual. The strongest UPO is in the range of  $m$  values 85–95 and it is the basic period (0.94–1.05 sec). The UPOs of a typical young normal case is shown in Fig. 6(a). The largest positive Lyapunov exponents of these UPOs are 2.27, 1.38, and 0.94, respectively. Their weights as given by the relative areas under these Gaussian curves are 77%, 13%, and 10%, respectively. The shortest UPO has  $m \sim 90$ , which we take as period 1. This is also the strongest. The other two UPOs are of period 2 and 3, with  $m \sim 180$  and 270, respectively. Since the sampling time is 0.011, period 1 corresponds to a recurrence time of nearly 0.99 sec, which is of the order of a normal heart rhythm. The physiological origin of the other two less dominant UPOs is not clear. The power spectrum of the normal ECG shows peaks at several frequencies [Fig. 3(a)]. In ECG second lead time series, the peak with maximum amplitude is called an  $R$  wave. The distance between two successive  $R$  waves is called an  $R$ - $R$  interval. It is known [42] that  $R$ - $R$  intervals in ECG signals are variable for the normal case.

Healthy old subjects are also characterized by three to four UPOs. Here the basic periodicity is in the range of  $m$  values 60–80 (0.66–0.88 sec), where as for young normal it is around 85–95. A typical case of this type is shown in the

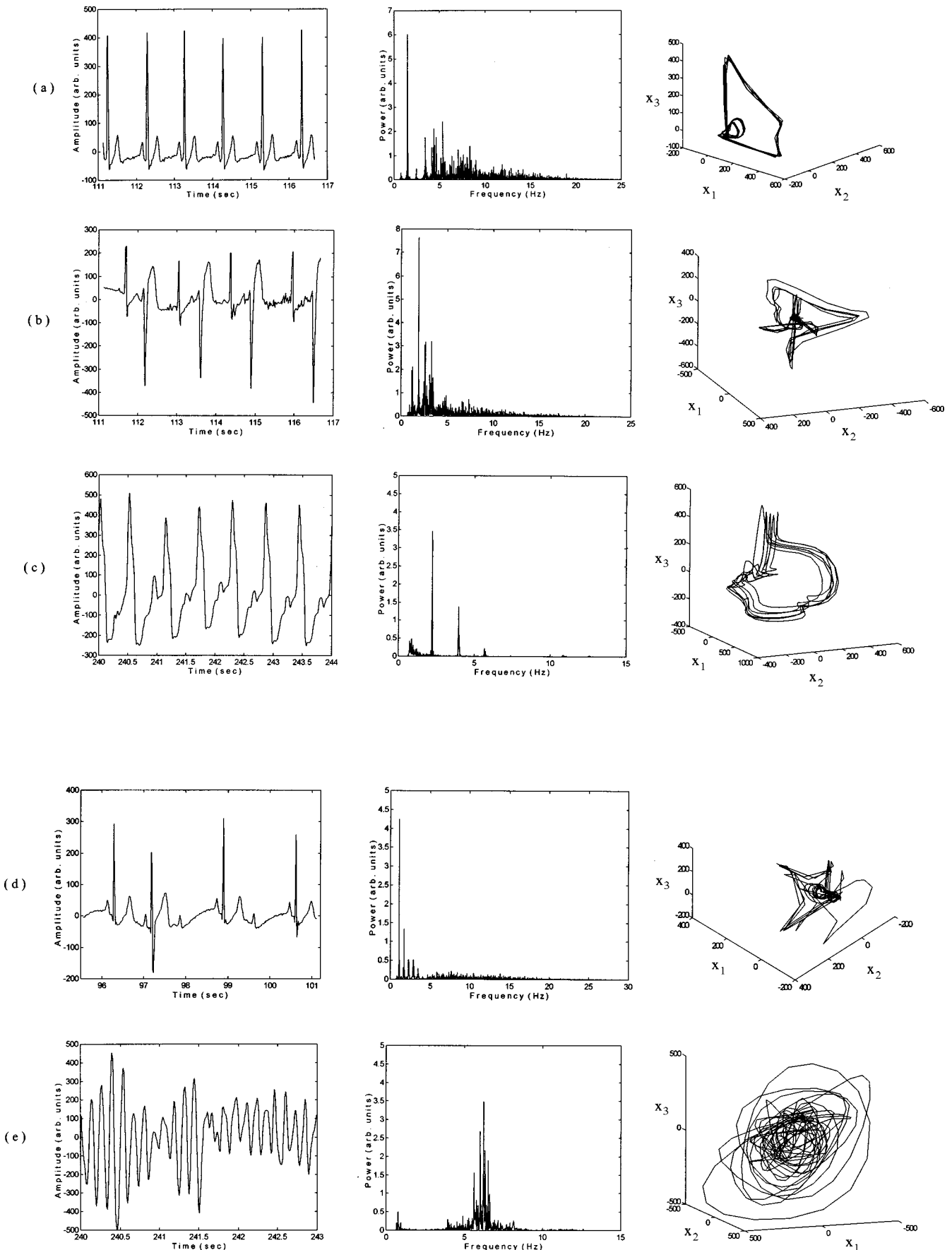


FIG. 3. ECG time series, power spectra, and attractor for typical (a) normal, (b) PVC, (c) VTA, (d) AV block, and (e) VF cases, respectively.  $x_1$ ,  $x_2$ , and  $x_3$  represent  $x(t)$ ,  $x(t + \tau)$ , and  $x(t + 2\tau)$  respectively, where  $x$  is the time series (arbitrary units) and  $\tau$  is the delay time in seconds.

TABLE II. Eigenvalue for individual periods and the largest positive Lyapunov exponent ( $\lambda$ ) for the whole system, for normal and pathological cases. In column 1 the entries within parentheses refer to the delay time  $\tau$  and radius  $\varepsilon$ , respectively. In column 3 the unit period ( $m = 1$ ) corresponds to 0.011 sec.

Subject	Period	$m$	Weight (%)	Eigenvalue	$\lambda$ (bits/sec)	Subject	Period	$m$	Weight (%)	Eigenvalue	$\lambda$ (bits/sec)	
<b>healthy young</b>	1 (0.04, 0.008)	1	91	77	4.91	(0.11, 0.0275)	4	160	14	4.29	1.60	
		2	180	13	6.86		5	196	13	5.67		
		3	275	10	7.44		7	285	6	4.35		
	2 (0.02, 0.015)	1	95	80	9.52	1.89	9	359	11	4.21	1.18	
		2	192	12	10.34		13	518	5	4.93		
		3	284	8	9.86		124	1	108	52		3.94
	3 (0.02, 0.02)	1	85	76	8.22	2.57	(0.04, 0.017)	2	216	24	4.05	1.45
		2	166	12	9.52			3	326	13	4.32	
		3	253	8	9.97			4	432	7	8.05	
		4	347	4	9.09			5	540	4	7.22	
	4 (0.03, 0.015)	1	87	72	9.04	2.81	<b>AV block MIT</b>	231	1	147	84	5.55
		2	174	18	9.15			2	285	16	11.50	
3		284	10	10.78	207			1	175	72	3.62	
<b>healthy old</b>	1 (0.03, 0.016)	1	80	70	3.73	(0.08, 0.02)	2	354	15	4.66	0.78	
		2	159	16	9.54		3	533	8	4.99		
		3	237	9	9.50		4	708	5	5.35		
		4	317	5	11.71		<b>VTA CUDB</b>	cu02	1	51		76
	2 (0.04, 0.013)	1	67	69	4.20	(0.13, 0.03)		2	103	10	3.10	2.18
2		139	16	4.86	3			153	6	3.60		
3		206	9	5.80	4			204	4	3.94		
3 (0.03, 0.02)	4	273	6	5.83	1.94	5		257	4	4.60	0.88	
	1	75	60	5.08		cu06	1	57	41	2.10		
	2	150	20	5.71		(0.07, 0.015)	2	115	14	2.23		
	3	227	12	4.82			3	173	11	2.64		
4	297	8	5.94	4	230		11	2.68				
4 (0.03, 0.03)	1	63	57	4.57	2.43	5	288	14	2.67	2.92		
	2	167	21	5.45		6	346	9	2.89			
	3	189	14	5.82		cu11	1	65	72		7.24	
	4	254	8	5.43		(0.07, 0.012)	2	132	14		9.63	
<b>PVC MIT</b>	107 (0.06, 0.04)	1	75	51	4.59		3	197	5	9.88	1.73	
		2	157	13	3.77		4	269	5	9.82		
		3	234	13	4.63	5	324	4	13.73			
	109 (0.04, 0.011)	4	302	6	5.43	1.67	cu13 (0.04, 0.015)	1	47	51	2.30	
		5	386	9	4.28			2	95	15	2.92	
		6	460	8	3.52			3	143	12	2.97	
106	1	62	61	4.29	2.50	<b>VF CUDB</b>	4	192	9	3.15	1.73	
	2	124	14	6.81			5	240	5	4.33		
	3	184	8	7.51			6	287	4	4.91		
	4	251	7	7.81			7	336	4	3.47		
	5	313	6	9.55			cu01	1	15	28		3.34
6	374	4	7.83	(0.04, 0.011)	2	30	15	4.38				

TABLE II. (Continued).

Subject	Period	$m$	Weight (%)	Eigenvalue	$\lambda$ (bits/sec)	Subject	Period	$m$	Weight (%)	Eigenvalue	$\lambda$ (bits/sec)				
0.03)	3	48	10	4.73	5.56	cu09 (0.06, 0.04)	16	719	4	9.56	1.90				
	4	61	9	4.74			17	757	4	6.71					
	5	74	7	4.76			1	36	9	7.12					
	6	93	6	5.10			2	80	26	5.71					
	7	103	6	4.08			3	120	7	5.61					
	8	117	6	5.60			4	161	11	6.10					
	9	145	4	4.89			5	202	7	6.02					
	10	169	4	4.76			6	243	9	5.56					
	11	184	5	4.78			7	291	3	6.13					
	cu03 (0.06, 0.015)	1	45	14			2.99	1.26	cu11 (0.03, 0.05)	8		324	15	5.59	4.19
		2	89	7			3.24			9		365	5	6.78	
3		135	7	3.43	10	405	5			5.83					
4		179	15	3.14	11	447	3			4.87					
5		222	9	3.96	1	15	27			2.97					
6		267	4	3.55	2	28	13			3.35					
7		312	5	3.96	3	42	6			4.06					
8		357	6	5.28	4	56	6			4.11					
9		402	5	4.32	5	77	7			3.93					
10		446	4	6.05	6	92	8			3.75					
11		490	3	5.84	7	106	7			2.98					
12		536	6	5.76	8	122	9			3.03					
13		579	3	5.34	9	129	7			3.29					
14		624	2	4.26	10	147	5			3.39					
15		672	2	9.68	11	164	5			3.27					

Fig. 6(b). In the aging process the walls of the blood vessels become thick and this leads to a slight decrease in the blood circulation. To compensate for this the heart will work faster, which results in the shift of UPOs to a lower value of recurrence time [43].

In sharp contrast to three to four UPOs for normal cardiac system, we find that a pathological case such as PVC contains significantly more UPOs of higher periods (approximately six UPOs). The basic period is usually the most

dominant and occurs in the wide range of  $m$  values 62–110 (0.68–1.22 sec) (see Table II). From the point of view of the attractor we can see that the PVC attractor has additional orbits compared to the healthy subject [Fig. 3(b)]. In fact, most of the other pathological cases also have additional orbits compared to normal subjects. In Fig. 7(b), we observe the occurrence of dominant UPOs from 3.33 to 5.55 sec for the PVC case, in addition to the UPOs of lower recurrence time values of 0.77–3.33 sec, which we find in the normal case.

In the normal heart, the impulse originating at the sinus node travels through an atrium, the atrio ventricular node, and then into the ventricles through a specialized conducting system consisting of the bundle of His and Purkinje fibers. The activity of the atria and ventricles are synchronized [19,44,45]. In PVC, this synchronization is lost, resulting in irregular and higher  $R$ - $R$  intervals [45]. The higher number of UPOs probably reflects this larger number of possible dynamical states in PVC, occurring at different sites of the cardiac system.

UPOs for the AV block are shifted to higher values of recurrence time depending on the degree of the block. UPOs for a 2:1 AV block are shown in Fig. 7(c). There are only two dominant UPOs with areas 84% and 16%. Here the basic periodicity is 147 (1.63 sec), which is much higher than the normal case. In AV block there is delay in the conduction of electrical impulses from the atrium to the atrio ventricular node [45]. As a result, ventricular stimulation is delayed. So we get UPOs at higher values of recurrence time.

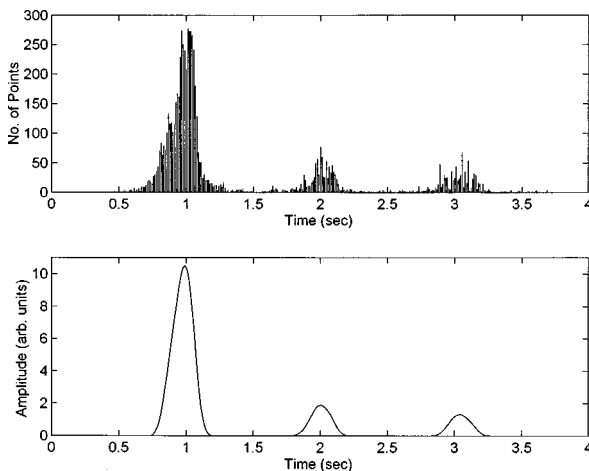


FIG. 4. UPOs of the healthy young subject (1). (a) Histogram and (b) its convolution. The relative intensities are given in Table II.

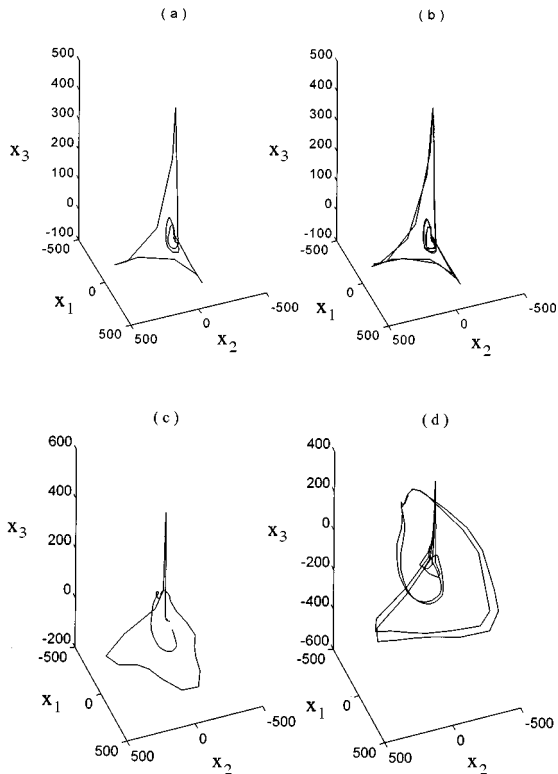


FIG. 5. Trajectories of periods 1 and 2 for a healthy subject: (a) period 1,  $m \sim 90$ ; (b) period 2,  $m \sim 180$ , and pathological PVC subject; (c) period 1,  $m \sim 75$ ; and (d) period 2,  $m \sim 150$ . In time units  $1 m = 0.011$  sec.  $x_1$ ,  $x_2$ , and  $x_3$  represent  $x(t)$ ,  $x(t + \tau)$ , and  $x(t + 2\tau)$ , respectively, where  $x$  is the time series (arbitrary units) and  $\tau$  is the delay time in seconds.

For VTA, there are five to seven dominant UPOs with the basic periodicity in the range of  $m$  values 45–65 (0.50–0.72 sec). UPOs are shifted to lower values of recurrence time compared to the normal (Fig. 8). UPOs of a typical VTA are shown in the Fig. 8(b). There are five dominant UPOs with areas of 76%, 10%, 6%, 4%, and 4%. Here the basic periodicity is  $m = 50$  (0.55 sec). VTA results from a rapidly discharging focus developed in the ventricular myocardium usually from a single focus [45]. It will not respond to the

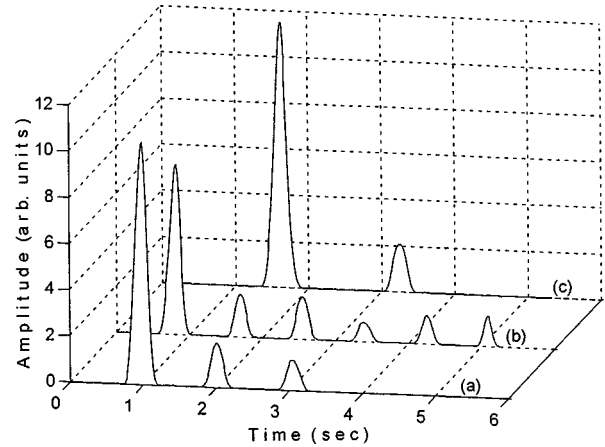


FIG. 7. Comparison of UPOs of (a) a healthy young subject (1), (b) PVC (107), and (c) AV block (231). Refer to Table II for the relative intensities of the UPOs.

sino atrial (SA) node and both of them act independently of each other. Thus VTA is the result of a reentry mechanism within the ventricular myocardium. Consequently, the UPOs are shifted towards the lower values of recurrence time. The cases of VF are found to have more than ten UPOs with a basic periodicity of  $m = 15-45$  (0.16–0.50 sec). The number of UPOs varies slightly, depending on the extent of fibrillation. A typical case is shown in Fig. 8(c). The area under the peaks are (25–30)%, 15%, 10%, 9%, 7%, 6%, 6%, 6%, 6%, 4%, 4%, and 5%. Here the basic periodicity is 21. In VF, rapidly discharging stimuli come from the single or multifoci within the ventricles [45]. As a result, ventricles cannot effectively respond to each stimulus from the SA node and its rate is rapid and irregular. So we get more UPOs with significantly lower values of recurrence time. The eigenvalues and the largest Lyapunov exponent of individual UPOs for four cases in each of the different cardiac conditions also are given in Table II. (Only two cases are given for AV block.)

**V. DIMENSION INDEPENDENCE AND STATIONARITY OF UPOs**

The distribution and the relative intensity (i.e., area under the peaks) of the UPOs of the cardiac system are essentially

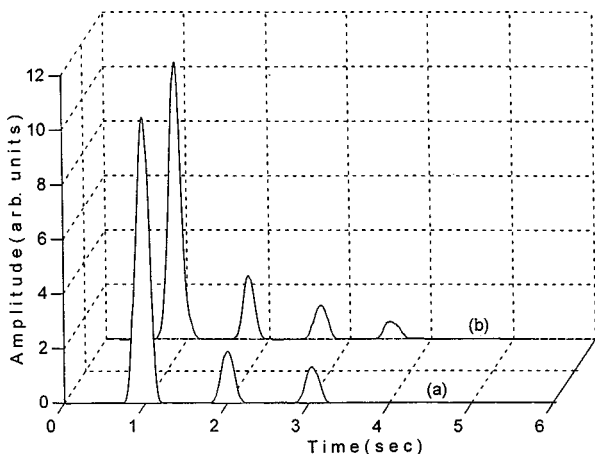


FIG. 6. Comparison of UPOs of (a) a healthy young subject (1) and (b) healthy old subject (1). Refer to Table II for the relative intensities of the UPOs.

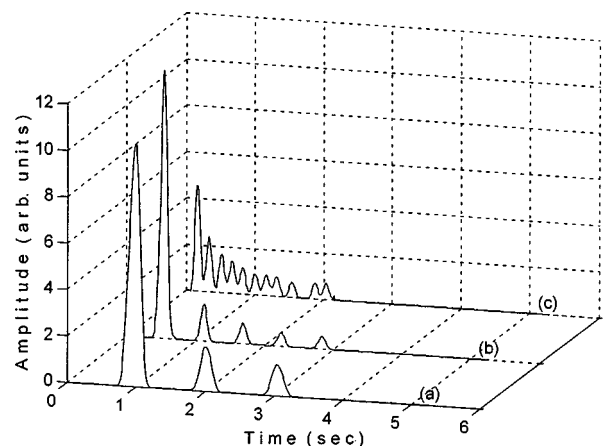


FIG. 8. Comparison of UPOs of (a) a healthy young subject (1), (b) VTA-cu02, and (c) VF-cu01. Refer to Table II for relative intensities of the UPOs.

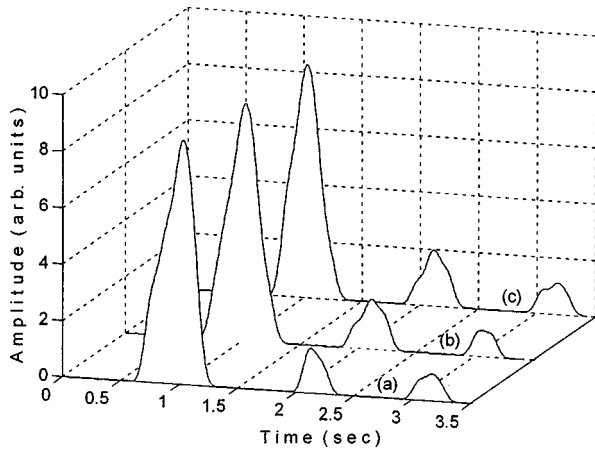


FIG. 9. Comparison of UPOs in various embedding dimensions  $d$  for a typical healthy subject: (a)  $d=3$  {80,12,8}, (b)  $d=5$  {77,16,7}, and (c)  $d=6$  {80,12,8}. Numbers in curly brackets give the relative intensities of the UPOs in the order of increasing values of the recurrence time.

invariant to increasing embedding dimension. The relative intensity (in percent) of the three UPOs for a healthy heart for embedding dimensions 3, 5, and 6 are (80,12,8), (77,16,7), and (80,12,8), respectively, with a basic periodicity of  $m=90$  (recurrence time of 1 sec). These results are shown in Figs. 9(a)–9(c). A similar analysis has been carried out for the PVC subject. These are shown in Figs. 10(a)–10(c). The intensity (in percent) for embedding dimensions 3, 5, and 6 are (51,13,13,6,9,8), (44,12,14,7,12,11), and (46,13,16,8,10,7), respectively. In all cases the recurrence time remains essentially the same. This clearly proves that UPOs are essentially insensitive to the embedding dimension and hence they are genuine returns [17].

Furthermore, there are no significant changes in the number of UPOs and their distribution when the UPO analysis is performed in different portions of the time series, which proves the stationary character of the ECG time series. The UPO analysis of the different portions of the time series of a

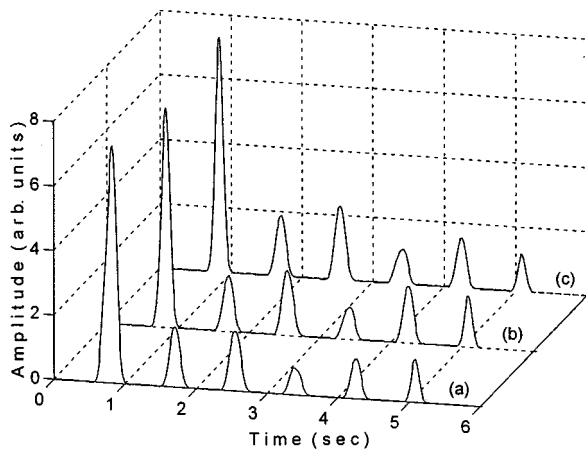


FIG. 10. Comparison of UPOs in various embedding dimension  $d$  for a typical pathological subject with PVC: (a)  $d=3$  {51,13,13,6,9,8}, (b)  $d=5$  {44,12,14,7,12,11}, and (c)  $d=6$  {46,13,16,8,10,7}. Numbers in curly brackets give the relative intensities of the UPOs in the order of increasing values of the recurrence time.

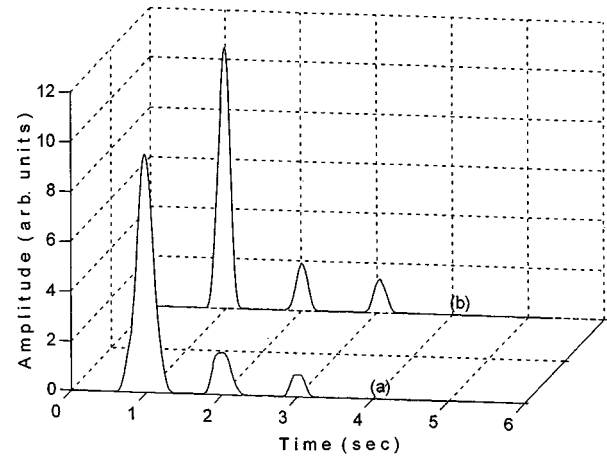


FIG. 11. Comparison of UPOs in different portions of time series for a normal subject: (a) portion 1 (first 10 000 data points) {77,13,10} and (b) portion 2 (the next 10 000 data points) {78,15,7}. Numbers in curly brackets give the relative intensities of the UPOs in the order of increasing values of the recurrence time.

typical normal time series are shown in Figs. 11(a) and 11(b) and that of PVC is shown in Figs. 12(a) and 12(b).

## VI. SURROGATE ANALYSIS OF UPOs

Finally, in order to assess the reliability of the observed UPOs, the UPO analysis is extended to its surrogate data. Since the surrogate data are the random representation of the original data, the surrogates are not expected to preserve the original UPO distribution [10]. The statistical significance of the frequency of occurrence of the patterns in the original UPOs can be tested by a comparison with the UPOs extracted from the surrogate data [18]. We can calculate the statistical measure  $S$  [18], which is given by  $S=(N - \langle N_s \rangle)/\sigma$ , where  $N$  is the value of the discriminating statistic for the original and  $N_s$  is that for the surrogate. Angular brackets and  $\sigma$  represent the mean and the standard deviation of  $N_s$ , respectively. Here the number of  $(m, \varepsilon)$  recurrence

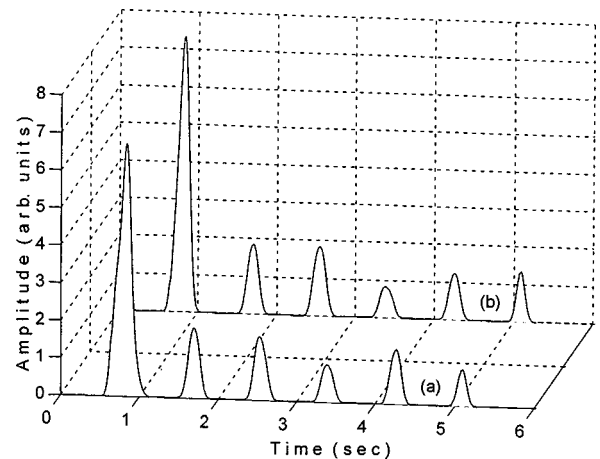


FIG. 12. Comparison of UPOs of a typical pathological subject with PVC in different portions of the time series: (a) portion 1 (first 10 000 data points) {51,13,13,6,9,8} and (b) portion 2 (the next 10 000 data points) {52,13,12,7,10,6}. Numbers in curly brackets give the relative intensities of UPOs with increasing values of the recurrence time.

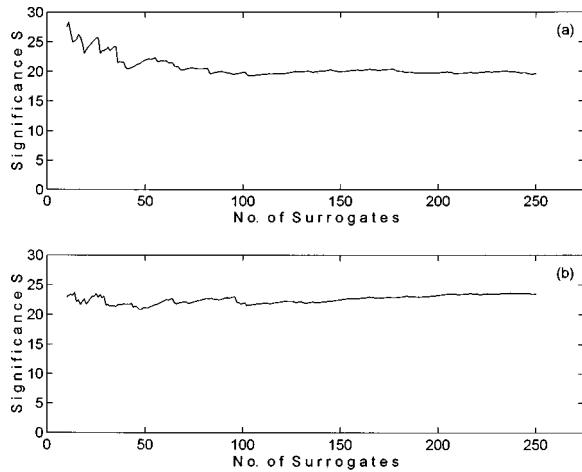


FIG. 13. Significance  $S$  (dimensionless) for a typical healthy subject: (a) Gaussian-scaled surrogate and (b) phase-randomized surrogate. See the text for the definition of  $S$ .

points of dominant UPOs is used as the discriminating statistic. For an UPO with a recurrence time  $m$ , we calculate  $S_m$ , which we define as  $S_m = (N_m - \langle N_s \rangle_m) / \sigma$ . From this, the significance  $S$  is obtained by the weighted average of  $S_m$ , where the weighting factor is the number of  $(m, \varepsilon)$  points. The number of surrogates was increased until the saturation of  $S$  is observed. (See Fig. 13 for a typical normal healthy case.) The significance  $S$  values for 250 surrogates in each case of normal, PVC, AV block, VTA, and VF for both phase-randomized surrogates and Gaussian-scaled random-phase surrogates are shown in the Table III.

It has been suggested that any value of  $S > 2$  indicates that the original data do not arise from a linear stochastic process [18]. The values obtained for each subject are greater than 2, indicating that a nonlinear structure is present in the dynamics producing the time series for all cases.

## VII. SUMMARY

In summary, we observe that neither the average exponent for the whole attractor nor the individual exponents of the UPOs have any noticeable regularity or distinction between

TABLE III. Significance  $S$  value of the UPOs of typical normal and pathological subjects for phase-randomized surrogates and Gaussian-scaled surrogates.

Subject	Phase-randomized surrogate	Gaussian-scaled surrogate
normal	$23.54 \pm 0.06$	$19.83 \pm 0.16$
PVC	$7.97 \pm 0.02$	$10.03 \pm 0.03$
AV block	$26.36 \pm 0.11$	$18.94 \pm 0.07$
VTA	$36.14 \pm 0.18$	$30.93 \pm 0.19$
VF	$4.75 \pm 0.01$	$4.95 \pm 0.01$

the normal and pathological cases. This is so even among the normal cases. Thus the exponents or the related dimensions cannot serve as a useful characterization of the cardiac system. Nor can the power spectrum be used to distinguish the states of the cardiac system since the spectra are quite complicated in both the normal and pathological cases.

The number and distribution in terms of periodicity and intensity of the UPOs, on the other hand, are seen to provide an unambiguous and quantitative characterization of the cardiac condition. The healthy heart is well characterized by three to four UPOs of well-defined recurrence time ranges. The recurrence time, intensity distribution, and number of UPOs for the various pathological conditions such as PVC, VTA, AV block, and VF are quite distinct and characteristic.

UPO analysis is shown to be robust in that UPOs are rather insensitive to embedding dimension and are stationary. Surrogate analysis indicates the nonlinear structure of the ECG time series with UPO distribution as the discriminating statistic and supports an earlier surrogate analysis with correlation dimension  $d_2$  as the discriminating factor. Knowledge of the Lyapunov exponents and the periodicity of the UPOs may be of help in the possible control of chaos in human cardiac systems.

## ACKNOWLEDGMENT

Financial assistance from the Department of Science and Technology of the Government of India (Grant No. SP/S1/H-23/95) is gratefully acknowledged.

- [1] C. Letellier, P. Dutertve, and B. Mahen, *Chaos* **5**, 271 (1995).
- [2] D. Pierson and F. Moss, *Phys. Rev. Lett.* **75**, 2124 (1995).
- [3] R. Marcinek and E. Pollock, *J. Chem. Phys.* **100**, 5894 (1994).
- [4] V. Franceschini, C. Giberti, and Z. Zheng, *Nonlinearity* **6**, 251 (1993).
- [5] B. Eckhardt and S. Grossman, *Phys. Rev. E* **50**, 4571 (1994).
- [6] D. P. Lathrop and E. J. Kostelich, *Phys. Rev. A* **40**, 4028 (1989).
- [7] D. Auerbach, P. Cvitanovic, J. P. Eckmann, G. Gunaratne, and I. Procaccia, *Phys. Rev. Lett.* **58**, 2387 (1987).
- [8] C. Grebogi, E. Ott, and J. A. Yorke, *Phys. Rev. A* **37**, 1711 (1988).
- [9] P. Cvitanovic, *Phys. Rev. Lett.* **61**, 2729 (1988).
- [10] P. So, E. Ott, S. J. Schiff, D. T. Kaplan, T. Sauer, and C. Grebogi, *Phys. Rev. Lett.* **76**, 4705 (1996).
- [11] E. Ott, C. Grebogi, and J. A. Yorke, *Phys. Rev. Lett.* **64**, 1196 (1990).
- [12] W. L. Ditto, S. N. Rauseo, and M. L. Spano, *Phys. Rev. Lett.* **65**, 3211 (1990).
- [13] E. R. Hunt, *Phys. Rev. Lett.* **67**, 1953 (1991).
- [14] V. Petrov, V. Gasper, J. Masere, and K. Showalter, *Nature (London)* **361**, 240 (1993).
- [15] R. W. Rollins, P. Parmananda, and P. Sherard, *Phys. Rev. E* **47**, R780 (1993).
- [16] S. J. Schiff, K. Jerger, D. H. Dueng, T. Chang, and M. L. Ditto, *Nature (London)* **370**, 615 (1994).
- [17] R. Badii, E. Brun, M. Finardi, L. Flepp, R. Holzner, J. Parisi, C. Reyl, and J. Simonet, *Rev. Mod. Phys.* **66**, 1389 (1994).
- [18] X. Pei and F. Moss, *Nature (London)* **379**, 619 (1996).
- [19] Leon Glass and D. Hunter, *Physica D* **43**, 1 (1993).

- [20] A. Babloyantz and A. Destexhe, *Biol. Cybern.* **58**, 203 (1988).
- [21] A. Casseloggio, A. Corana, and S. Ridella, *Chaos Solitons Fractals* **5**, 713 (1995).
- [22] E. J. Kostelich and T. Schreiber, *Phys. Rev. E* **48**, 1752 (1993).
- [23] T. Schreiber, *Phys. Rev. E* **48**, R13 (1993).
- [24] P. Grassberger, R. Hegger, H. Kantz, and C. Schattatratte, *Chaos* **3**, 127 (1993).
- [25] A. Garfinkel, M. L. Spano, W. L. Spano, W. L. Ditto, and J. N. Weiss, *Science* **257**, 1230 (1992).
- [26] K. Hall, D. J. Christini, M. Tremblay, J. J. Collins, L. Glass, and J. Billette, *Phys. Rev. Lett.* **78**, 4518 (1997).
- [27] A. Roy, T. W. Murphy, T. D. Maior, Z. Gills, and E. R. Hunt, *Phys. Rev. Lett.* **8**, 1259 (1992).
- [28] P. So, E. Ott, T. Sauer, B. J. Gluckman, C. Grebogi, and S. J. Schiff, *Phys. Rev. E* **55**, 5398 (1997).
- [29] A. M. Albano, J. Muench, C. Schwartz, A. I. Mees, and P. E. Rapp, *Phys. Rev. A* **38**, 3017 (1988).
- [30] A. Wolf, J. B. Swift, H. W. Swinney, and J. A. Vastano, *Physica D* **16**, 285 (1985).
- [31] M. Möller, W. Lange, F. Mitschke, and W. B. Abraham, *Phys. Lett. A* **138**, 176 (1988).
- [32] R. Badii, G. Broggi, B. Derighetti, M. Ravani, S. Ciliberto, A. Politi, and M. A. Rubio, *Phys. Rev. Lett.* **60**, 979 (1988).
- [33] K. Fraedrich and R. Wang, *Physica D* **65**, 393 (1993).
- [34] J. Theiler and S. Eubank, *Chaos* **3**, 771 (1993).
- [35] P. Grassberger and I. Procaccia, *Physica D* **9**, 189 (1983).
- [36] J. H. Lefebvre, D. A. Goodings, M. V. Kamath, and E. Z. Fallen, *Chaos* **3**, 267 (1993).
- [37] G. Sugihara and R. M. May, *Nature (London)* **344**, 734 (1990).
- [38] R. B. Govindan, K. Narayanan, and M. S. Gopinathan, *Chaos* (to be published).
- [39] J. Theiler, S. Eubank, A. Longtin, B. Galdrikian, and J. D. Farmer, *Physica D* **58**, 77 (1992).
- [40] P. E. Rapp, A. M. Albano, I. D. Zimmerman, and M. A. Jimenez-Monntano, *Phys. Lett. A* **192**, 27 (1994).
- [41] The MIT-BIH Arrhythmia Database CD-ROM, 2nd ed. (Harvard-MIT Division of Health Sciences and Technology, Cambridge, MA, 1992).
- [42] A. L. Goldberger, B. R. Rigney, and B. J. West, *Sci. Am.* **262**, 34 (2) (1990).
- [43] We are grateful to Dr. S. Thanikachalam of the Cardiac Care Center, Ramachandra Medical College, Chennai for this interpretation and other useful discussions.
- [44] L. Glass, *Phys. Today* **49** (8), 40 (1990).
- [45] M. J. Goldman, *Principles of Electrocardiography* (Lange Medical Publications, Singapore, 1973).